Supporting Information for

Structural Examination of the Transient 3-Aminotyrosyl Radical on the PCET Pathway of *E. coli* Ribonucleotide Reductase by Multifrequency EPR Spectroscopy

Mohammad R. Seyedsayamdost,[†,&] Tomislav Argirevic,[§] Ellen C. Minnihan,[†] JoAnne Stubbe*[†,‡] and Marina Bennati*[§]

Department of Chemistry[†] and Biology[‡], Massachusetts Institute of Technology, 77 Massachusetts Avenue, Cambridge, MA 02139-4307, and Max Planck Institute for Biophysical Chemistry[§], 37077 Göttingen, Germany

Marina.Bennati@mpibpc.mpg.de

[&]*Current address: Department of Biological Chemistry and Molecular Pharmacology, 240 Longwood Avenue, C1-609, Boston, MA 02115*

Table S1. Summary of EPR parameters (in MHz)[a] previously reported for an *o*-aminophenol radical.[b]

Entry	Reference	g factor	$^b\text{A}_3^\text{H}$	$^b\text{A}_4^\text{H}$	$^b\text{A}_5^\text{H}$	$^b\text{A}_6^\text{H}$	$^b\text{A}^\text{N}$	$^b\text{A}^\text{N-H}$
1	Neta *et al.*[c]	2.00372	<0.28	12.1	2.8	8.2	13.3	14.8 (2)[d]
2	Loth *et al.*[e]	nr[f]	1.29	6.5	1.5	6.1	12.4	21.3/16.2
3	Loth *et al.*[f]	nr[f]	0.28	8.4	3.9	7.0	12.6	19.3/15.4

[a] Hyperfine coupling constants were reported in Gauss, they have been converted to MHz as per 1 G=2.8 MHz. [b] See Figure S1 for numbering scheme of *o*-aminophenol radical. A_x^H is the hyperfine coupling constant from the proton attached to C_x of the *o*-aminophenol radical. A^N is the coupling from the N–nucleus, $\text{A}^\text{N-H}$ is the coupling from the amine protons. [c] Generated by in situ radiolysis/EPR spectroscopy in water at room temperature (Ref. 36). [d] Two protons with identical hyperfine splitting constants. [e] Spectra obtained in CH_2Cl_2/THF at −61°C (Ref. 41). [f] Spectra obtained in CH_3OH at −75°C (Ref. 41).

Table S2. UV spectral properties of authentic [^{14}N]-NH$_2$Y[a] and synthetic [^{15}N]-NH$_2$Y determined in H_2O at 25°C.

Protonation Form	Authentic NH$_2$Y λ_{max} (nm)[b], ε (M^{-1}cm^{-1})[c]	Synthetic ^{15}N-NH$_2$Y λ_{max} (nm), ε (M^{-1}cm^{-1})[c]
H_3N^+−Y	275 ± 1, 2150 ± 150	275 ± 1, 1900 ± 130
H_2N−Y	289 ± 1, 3200 ± 220	289 ± 1, 3200 ± 220
H_2N−Y$^-$	303 ± 1, 5100 ± 360	303 ± 1, 4700 ± 330

[a] "Authentic" [^{14}N]-NH$_2$Y was obtained from Sigma-Aldrich. [b] Estimated error based on accuracy of spectrophotometer. [c] Estimated error based on accuracy of spectrophotometer and microbalance weight measurements.
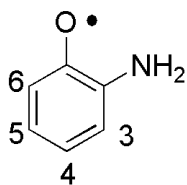
Figure S1. Numbering scheme for the spectral data on the *o*-aminophenol radical data in Table S1. Accordingly, A_3^H in Table S1 corresponds to the hyperfine coupling constant from the proton attached to C_3.
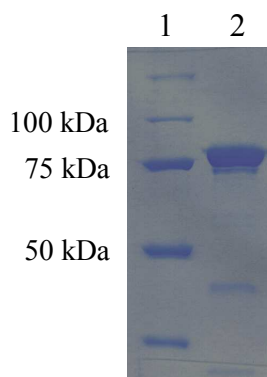

Figure S2. SDS PAGE analysis of purified $[^{15}N]$-NH$_2$Y$_{730}$-α2. Lane (1), MW marker. The MW for the relevant bands is indicated. Lane (2), purified Y$_{730}$NH$_2$Y-α2 (5 μg).
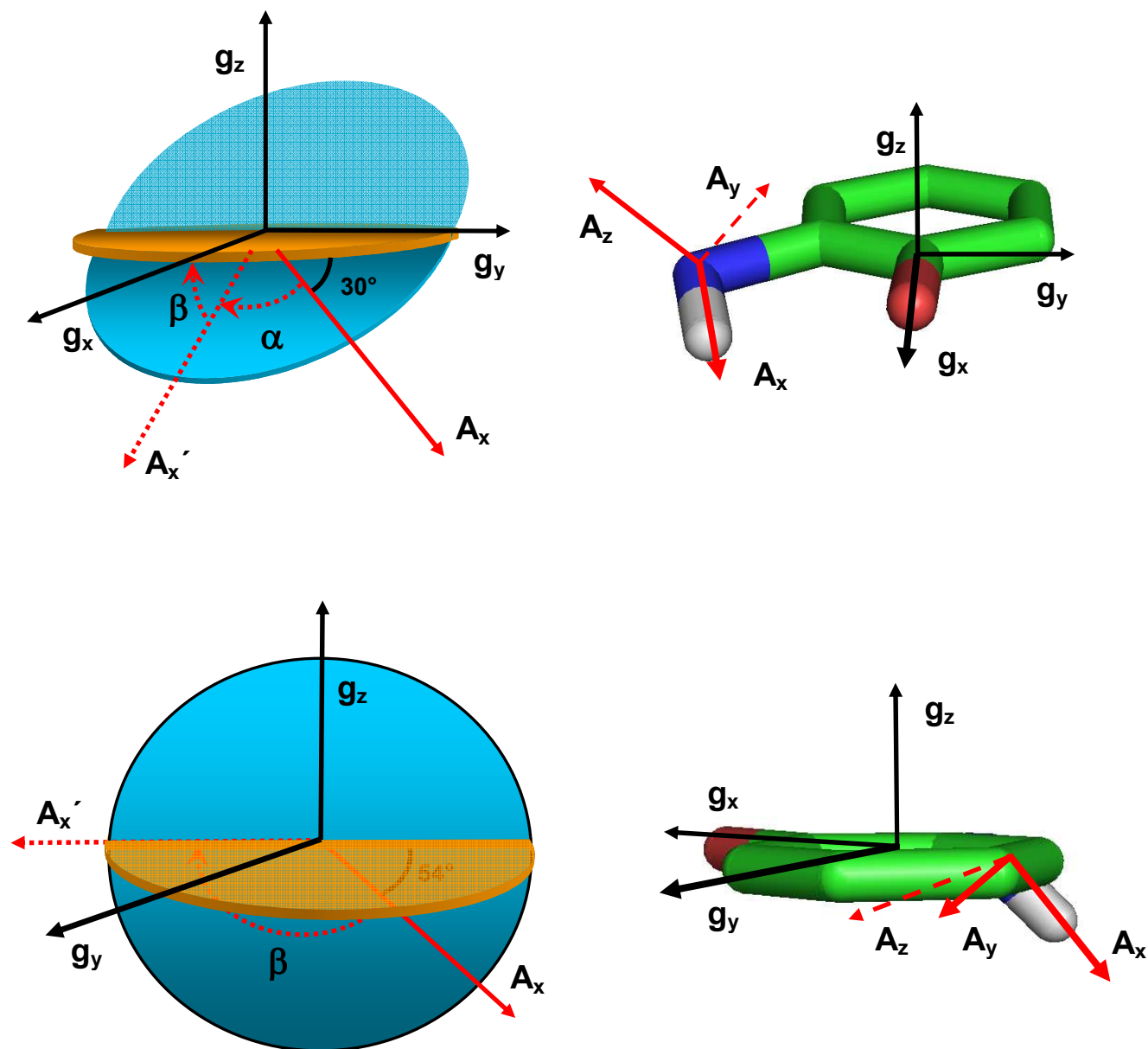
Figure S3. Euler rotations and A tensors for N-H(1) (top) and N-H(2) (bottom). (Top) Two rotations are required to co-linearize the A and g tensor axes. The first rotation occurs about A_z (Euler angle α, here negative) and generates A_x' co-linearizing g_y and A_y. The second rotation occurs about A_y' (or g_y) and corresponds to Euler angle β (here also negative). This leads to co-linear g_x/A_x and g_z/A_z axes. (B) In case of N-H(2), the first rotation occurs about A_y and moves A_x to A_x' (Euler angle β, here negative). The second rotation occurs about A_z (Euler angle γ, here negative). See Table 1 for values of α, β and γ for each proton. The negative values of the angles are due to the requirement of counter-clockwise rotations in the Euler convention. For clarity, the translation of the other tensor axes after each rotation is not shown (i.e. A_y' and A_z').
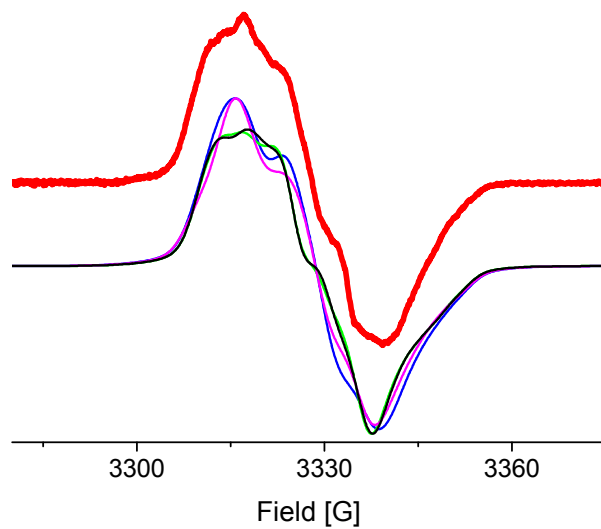
Figure S4: Simulations of the 9 GHz CW-EPR spectrum of $[^{15}N]$-NH$_2$Y$_{730}\bullet$ for the four possible combinations of the β angle signs for the two NH$_2$ protons, i.e. ++ (green), +- (blue), -+ (magenta), -- (black). The red bold trace is the observed 9 GHz spectrum of $[^{15}N]$-NH$_2$Y$_{730}\bullet$ in protonated buffer.
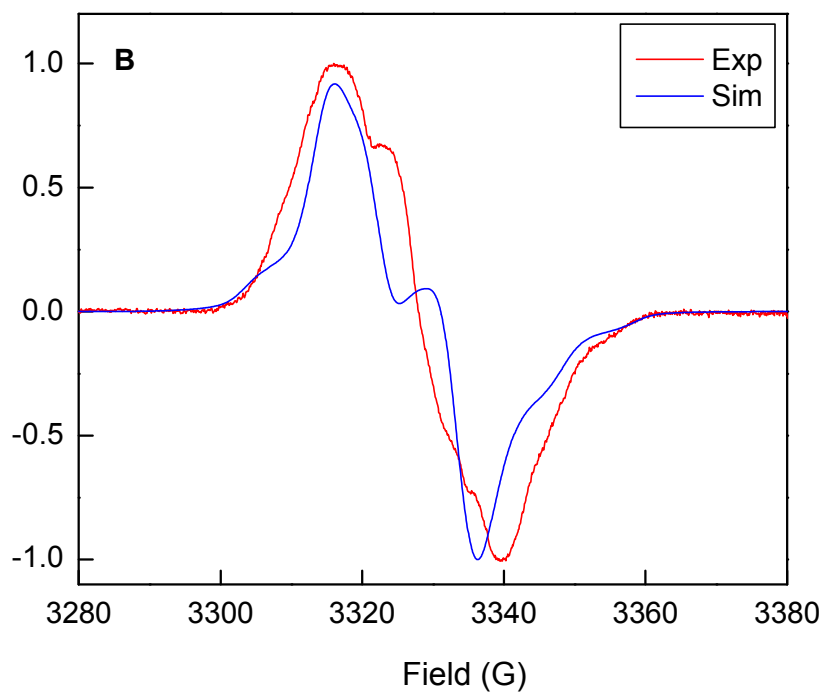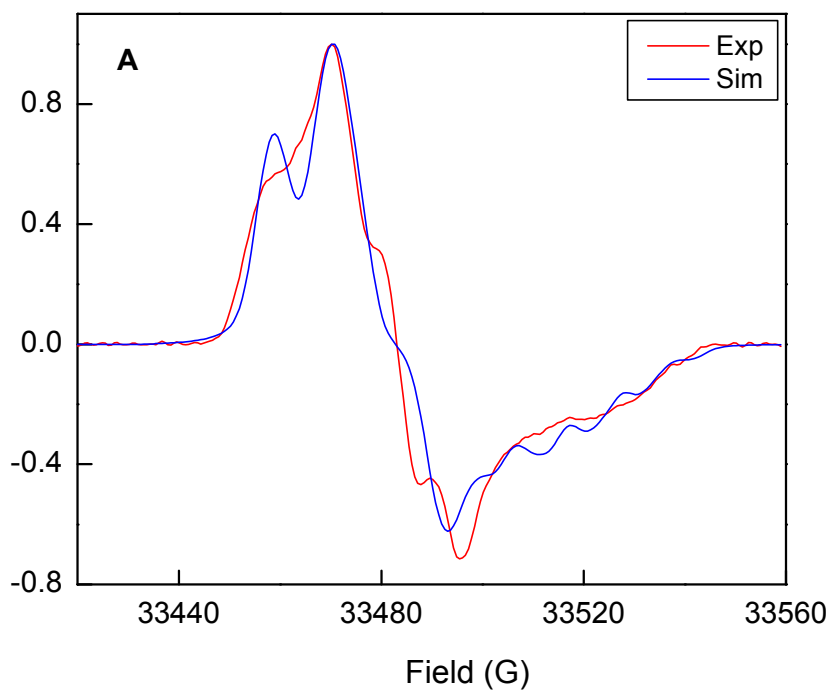
Figure S5: Observed 94 GHz (A) and 9 GHz (B) EPR spectrum of $[^{14}N]$-NH_2Y_{730}•-α2 (red trace) and computation of the spectrum of an ideal *sp2*-hybridized nitrogen in NH_2Y• (blue trace). The poor simulation of the data here contrasts to those in Figs. 5-7, where an *sp3*-hybridized nitrogen was used.

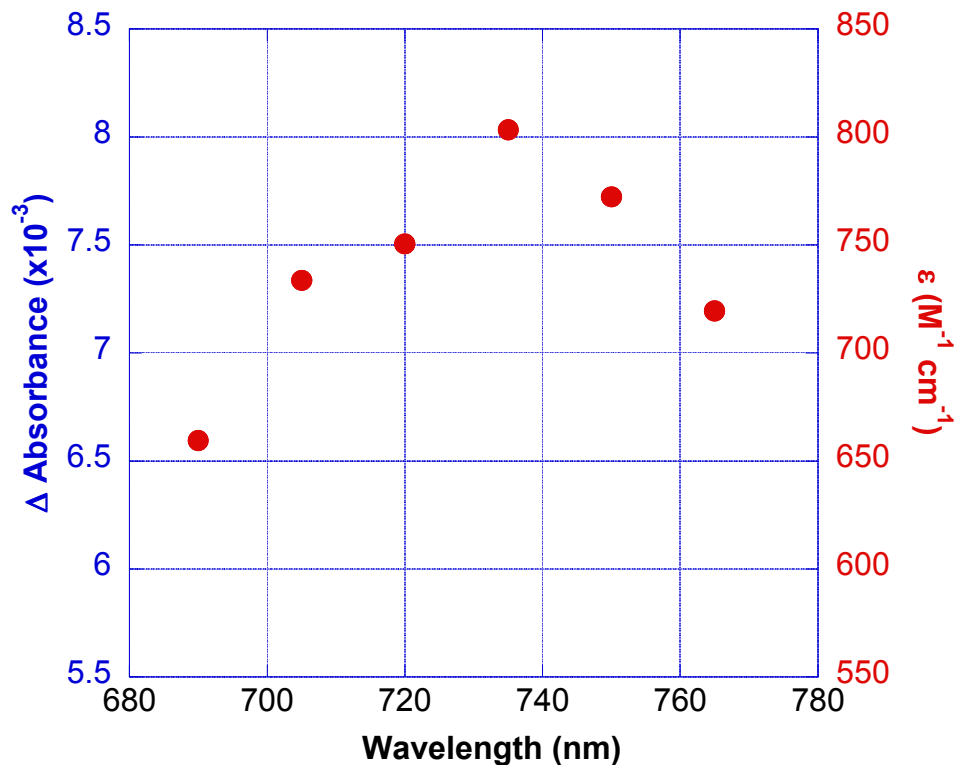**Figure S6.** Spectral reconstruction of the UV-vis spectrum of the broad, long wavelength feature observed upon stopped-flow reaction of $Y_{730}NH_2Y$-a2 with β2, CDP, and ATP. $Y_{730}NH_2Y$-a2 and ATP were rapidly mixed with β2 and CDP in a 1:1 ratio to give final concentrations of 30 μM, 3 mM, 30 μM, and 1 mM, respectively. Reactions were conducted at 25 °C and monitored over 5 seconds in 15 nm intervals. At each wavelength, kinetic traces were averaged and fit bi-exponentially. The total change in absorbance over the timecourse (left axis, blue) was used to determine approximate extinction coefficients (right axis, red) by determining the amount of NH_2Y• formed under identical experimental conditions and assuming that the broad, long-wavelength feature and NH_2Y• form in an equimolar ratio.
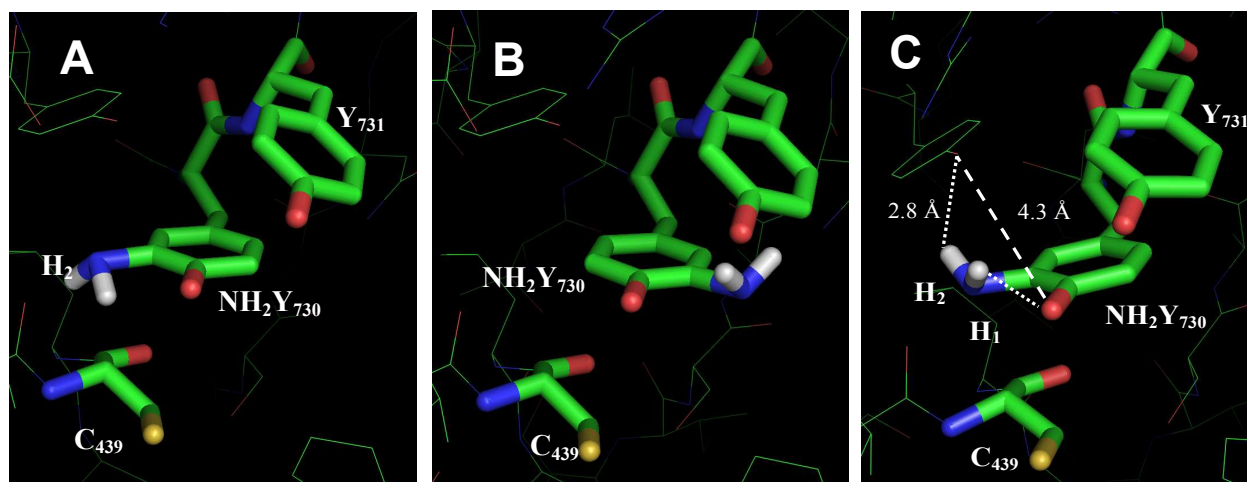
Figure S7: Models of the $Y_{731}-NH_2Y_{730}-C_{439}$ pathway. These orientations are consistent with the EPR data, but result in steric clashes within $\alpha 2$ and are inconsistent with recent structural data. In (A) the amino group is sterically hindered by the backbone carbonyl of L_{438} (the distance to H_2 is 1.7 Å) and in (B) it is too close to residue Y731. (C) is inconsistent with the recent structure of NH_2Y-$\alpha 2$ or NO_2Y-$\alpha 2$ (Uhlin & Stubbe, unpublished results).
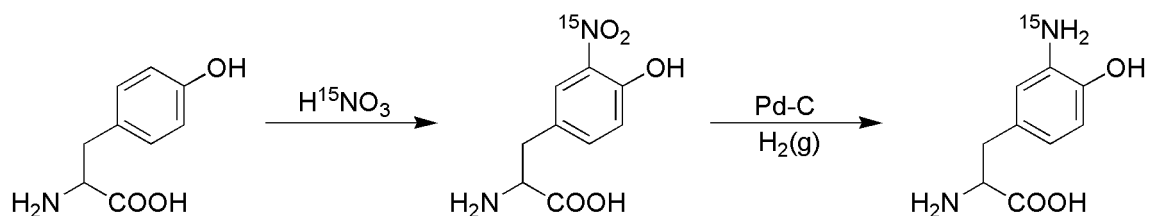
Scheme S1. Synthetic scheme used for preparation of $[^{15}N]$-NH_2Y. See Methods for details.
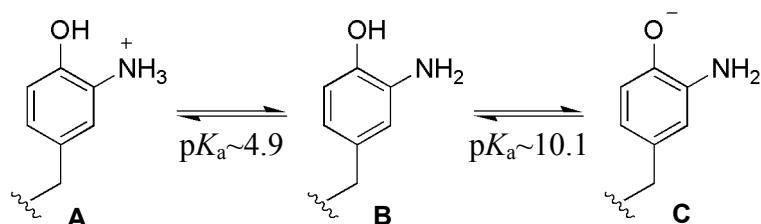
Scheme S2. Different protonation states and pK_as of NH_2Y. Species A, B, and C have absorption maxima at 275, 289, and 303 nm, respectively. The pK_as for conversion of A to B and B to C are from Refs. 31 and 32.